

Clustering in globally coupled phase oscillators

D. Golomb

Racah Institute of Physics, The Hebrew University, Jerusalem 91904, Israel

D. Hansel

*Racah Institute of Physics, The Hebrew University, Jerusalem 91904, Israel
and Centre de Physique Théorique, Ecole Polytechnique, 91128 Palaiseau, CEDEX, France*

B. Shraiman

AT&T Bell Laboratories, 600 Mountain Avenue, Murray Hill, New Jersey 07974

H. Sompolinsky*

*Racah Institute of Physics, The Hebrew University, Jerusalem 91904, Israel
and AT&T Bell Laboratories, 600 Mountain Avenue, Murray Hill, New Jersey 07974*

(Received 30 May 1991; revised manuscript received 5 September 1991)

A model of many globally coupled phase oscillators is studied by analytical and numerical methods. Each oscillator is coupled to all the other oscillators via a global driving force that takes the form $\sum_j g(\phi_j)$, where $g(\phi_j)$ is a periodic function of the j th phase. The spatiotemporal properties of the attractors in various regions of parameter space are analyzed. In addition to simple spatially uniform fixed points and limit cycles, the system also exhibits spatially nonuniform attractors of three kinds. First, there are cluster states in which the system breaks into a few macroscopically big clusters, each of which is fully synchronized. Second, there is a stationary state with full frequency locking but no phase locking. The distribution of phases is stationary in time. Third, in an extremely narrow regime of parameters, a nonperiodic attractor exists. It is found that the cluster state is stable to the addition of weak stochastic noise. Increasing the level of noise beyond a critical value generates a continuous transition to a stationary ergodic state. In the special case where the nonlinearities in the dynamics involve only first harmonics, *marginal states* are observed, characterized by a continuum of marginally stable limit trajectories. These states are unstable under the introduction of noise.

PACS number(s): 05.45.+b, 05.90.+m, 87.10.+e

I. INTRODUCTION

Many systems in physics, chemistry, and biology can be described as populations of coupled oscillators [1]. Examples are charge-density waves [2], some chemical-reaction systems [1], and oscillatory neuronal systems [3]. Understanding the cooperative dynamical properties of such systems is therefore of considerable theoretical and experimental interest. The conditions under which such populations exhibit synchronized activity have attracted renewed attention because of the recent discovery of synchronized oscillatory neuronal responses in the cat visual cortex [3,4].

Models of coupled oscillators have been studied by Kuramoto and co-workers [1,5,6] and others [7-9]. It has been shown that limit-cycle oscillators with weak coupling can be described by a system of *phase oscillators* where each individual oscillator is described by a single variable, its phase. The form of the phase equations is

$$\dot{\phi}_i = \omega_i + \sum_{j=1}^N K_{ij} \Gamma(\phi_i - \phi_j + \phi_{ij}^0), \quad i=1, \dots, N, \quad (1.1)$$

where ϕ_i denotes the phase of the i th oscillator and ω_i its local frequency, i.e., its frequency in the absence of in-

teraction between the oscillators. The last term represents the interaction between phases. The coefficients K_{ij} are the coupling strengths between pairs (i, j) , $\Gamma(\phi)$ is a periodic function of ϕ , and ϕ_{ij}^0 are fixed phase shifts. Thus, in the weak-coupling limit, the pairwise interaction are *synchronizing* interactions: They depend only on the phase *difference* of pairs of oscillators and tend to pin these differences to the values ϕ_{ij}^0 . Important work has been done on understanding the behavior of such a phase model, including the effect of stochastic and quenched fluctuations in the frequencies ω_i [1,5-9] and stochastic external noise [10]. Most of these studies focus on the mean-field case, where all pairs are interacting with equal strength:

$$K_{ij} = K/N, \quad i \neq j. \quad (1.2)$$

In cases of strong interactions between limit-cycle oscillators, the simple phase model [Eq. (1.1)] may not be appropriate. Even within a phase description, one expects important deviations in the form of nonlinear local terms [10], as well as interactions that depend on the states of the interacting oscillators and not just their phase differences.

In this work we study phase equations of the form

$$\dot{\phi}_i = \omega + f(\phi_i) - \sum_{j=1}^N K_{ij} g(\phi_j), \quad i=1, \dots, N, \quad (1.3)$$

where f and g are periodic functions. Unlike the model of Kuramoto and co-workers, the local phase oscillators are not simple rotators, but may exhibit a rich variety of behavior, depending on the structure of f . In addition, the interaction term is a driving force that does not depend on the phase of the driven oscillators. We will study only the case of global coupling; i.e., we will assume Eq. (1.2). In our case this implies that the driving force on each oscillator is equal. We shall focus here on the long-time behavior of this model in the limit of large N .

A special case of the phase model [Eq. (1.3)], appropriate for linear Josephson-junction arrays, has been studied recently [11]. This case corresponds to $f(\phi) = A \sin\phi$ and $g(\phi) = \sigma \sin\phi$. As we shall find, these special cases are highly non-generic. This nongeneric behavior may be associated in part with the generalized time-reversal symmetry that the above equations exhibit for this choice of f and g , as discussed in [12]. One of the goals of the present study is to try to characterize the nature of the long-time properties of this model for general forms of f and g , where no special symmetry exists. In particular, we will be interested in finding whether nontrivial spatio-temporal structures appear in such a model despite the global nature of the interaction.

A related model is the globally-coupled-map model studied by Kaneko [13]. The main difference is that in our case the local degrees of freedom are much simpler (in the absence of interactions) and in particular cannot exhibit chaotic motion. In fact, we find that the coupled-phase system does exhibit nonperiodic temporal behavior, but only in restricted regimes in parameter space. Nevertheless, some aspects of the collective dynamics found in the present model occur also in the case of coupled maps. In particular, we find that the system often spontaneously breaks into macroscopic clusters of coherent oscillating phases. These clusters are similar to the clusters found in [13], for globally coupled logistic maps, and in [14], for coupled maps in the vicinity of a single-map period-doubling bifurcation.

The paper is organized as follows. In Sec. II the model is presented and the different possible attractors of its collective dynamics are characterized. In Sec. III the properties of several explicit forms of the functions f and g are analyzed. These forms are characterized by the number of harmonic terms contained in their Fourier expansion. We first study the special case of f and g containing only the first harmonics. In this case a large regime of parameters exhibits a huge marginality: There is a continuous manifold of marginally stable limiting trajectories. The marginality is resolved by adding more Fourier components to the dynamics. We show that, in the generic case, the system possesses mainly two *spatially inhomogeneous* limit-cycle attractors: (1) an attractor where the phases group in macroscopic clusters, each of which consists of fully synchronized phases, in which all the rotators have the same phase, and (2) an attractor where the oscillating phases form a continuous time-

independent distribution. As mentioned above, we also find, in a narrow regime, attractors characterized by a continuous nonperiodic time-dependent distribution of phases. Also, the properties of the simple *spatially homogeneous* fixed points and limit cycles are studied. In Sec. IV we study the effect of adding external stochastic noise, analogous to thermal noise. The results are discussed in Sec. V.

II. MODEL AND THE ATTRACTORS

A. Model of coupled oscillators

We consider a system of N oscillators. The state of each oscillator is characterized by a phase ϕ_i , $0 \leq \phi_i < 2\pi$, $i=1, \dots, N$. The state of the system will be described by the vector $\boldsymbol{\phi} = \{\phi_i\}_{i=1, \dots, N}$. The equations of motion for the phases are assumed to be of the form

$$\dot{\phi}_i = \omega + f(\phi_i) - \frac{1}{N} \sum_{j=1}^N g(\phi_j), \quad i=1, \dots, N, \quad (2.1)$$

where f and g are continuous and periodic functions: $f(\phi) = f(\phi + 2\pi)$, $g(\phi) = g(\phi + 2\pi)$.

These equations describe a system of globally coupled oscillators. In the absence of coupling, the (free) motion of each oscillator obeys $\dot{\phi}_i = \omega + f(\phi_i)$. Thus, at large times, the trajectory of a free oscillator converges to a limit cycle or a fixed point. The global coupling is an additive term which is the same for all the oscillators.

The functions $f(\phi)$ and $g(\phi)$ are parametrized by their Fourier expansions, namely,

$$\begin{aligned} f(\phi) &= \sum_{n=1}^{\infty} A_n \sin(n\phi + \psi_n), \\ g(\phi) &= \sum_{n=1}^{\infty} \sigma_n \sin(n\phi + \alpha_n). \end{aligned} \quad (2.2)$$

Our main quantitative results will be presented for f containing up to three harmonics and g containing only its first harmonic. On the basis of these results, we will draw conclusions regarding the *generic* behavior of a system of equations of the form (2.1).

An important quantity characterizing the properties of our system is the single-phase distribution function defined by

$$P_N(\phi, t) = \frac{1}{N} \sum_{i=1}^N \delta(\phi - \phi_i). \quad (2.3)$$

We are interested in the behavior of the system in the limit of large N . The $N \rightarrow \infty$ limit of $P_N(\phi, t)$, defined by

$$P(\phi, t) \equiv \lim_{N \rightarrow \infty} P_N(\phi), \quad (2.4)$$

obeys the continuity equation [15]

$$\frac{\partial}{\partial t} P(\phi, t) + \frac{\partial}{\partial \phi} \{ [\bar{\omega}(t) + f(\phi)] P(\phi, t) \} = 0, \quad (2.5)$$

where

$$\bar{\omega}(t) \equiv \omega - \int_0^{2\pi} P(\phi', t) g(\phi') d\phi'. \quad (2.6)$$

The solution $P(\phi, t)$ must satisfy the periodicity condition

$$P(2\pi, t) = P(0, t) \quad (2.7)$$

and the normalization condition

$$\int_0^{2\pi} d\phi P(\phi, t) = 1. \quad (2.8)$$

It must also be non-negative,

$$P(\phi, t) \geq 0, \quad \forall \phi, t. \quad (2.9)$$

From the point of view of distribution functions, the model can be interpreted as a system of particles that move on the circumference of a circle. The velocity $v(\phi, t)$ of a particle with position ϕ depends on its position and on the position of all the other particles:

$$v(\phi, t) = \omega + f(\phi) - \int_0^{2\pi} P(\phi', t) g(\phi) d\phi'. \quad (2.10)$$

The ‘‘current’’ $J(\phi, t)$ of particles through a point ϕ is

$$J(\phi, t) = P(\phi, t) v(\phi, t). \quad (2.11)$$

B. Stability of solutions

A trajectory $\phi_0(t)$ is stable if every sufficiently small perturbation in the initial conditions $\delta\phi(0)$ decays to zero at large times. Focusing on linear stability, the evolution of the perturbation $\delta\phi(t)$ is given by

$$\frac{d(\delta\phi)}{dt} = M(\phi_0(t)) \delta\phi(t), \quad (2.12)$$

where the stability matrix M_{ij} is

$$M_{ij}(\phi) = \frac{\partial f(\phi_i)}{\partial \phi_i} \delta_{i,j} - \frac{1}{N} \frac{\partial g(\phi_j)}{\partial \phi_j}. \quad (2.13)$$

The solution of Eq. (2.12) is $\delta\phi(t) = U(t) \delta\phi(0)$, where the operator $U(t)$ is

$$U(t) \equiv T \exp \left[\int_0^t dt' M(\phi_0(t')) \right]. \quad (2.14)$$

The symbol T denotes the time-ordering operator. The trajectory $\phi(t)$ is stable if the norm of $U(t)$ decays exponentially with t .

For two cases, a fixed point and a limit cycle, this stability criterion can be put in a more explicit form. In the case of a fixed point, $\phi_0(t) = \phi_0$ and

$$U(t) = e^{M(\phi_0)t}. \quad (2.15)$$

Thus the fixed point (FP) is stable if all the eigenvalues of M have negative real parts. In the case of a limit cycle with time period T_p , the perturbation $\delta\phi$ after n_p periods is

$$\delta\phi(n_p T_p) = [U(T_p)]^{n_p} \delta\phi(0). \quad (2.16)$$

The limit cycle (LC) is stable if all the absolute values of the eigenvalues of $U(T_p)$ are smaller than 1, except for the eigenvalue which is associated with a perturbation $\delta\phi$ along the limit cycle, which is equal to 1.

When the distribution function $P(\phi, t)$ is continuous, it is sometimes more convenient to discuss the stability of

the system in terms of this function. The temporal evolution of an infinitesimal perturbation $\delta P(\phi, t)$ of $P(\phi, t)$ is given by

$$\frac{\partial[\delta P(\phi, t)]}{\partial t} = L(P) \delta P(\phi, t), \quad (2.17)$$

where the operator $L(P)$ is

$$\begin{aligned} L(P) \delta P(\phi, t) = & - \frac{\partial}{\partial \phi} \{ [\bar{\omega}(t) + f(\phi)] \delta P(\phi, t) \} \\ & + \frac{\partial P(\phi, t)}{\partial \phi} \int_0^{2\pi} d\phi' g(\phi') \delta P(\phi', t). \end{aligned} \quad (2.18)$$

The solution of Eq. (2.17) is $\delta P(\phi, t) = V(t) \delta P(\phi, 0)$, where the operator $V(t)$ is

$$V(t) = T \exp \left[\int_0^t dt' L(P(t')) \right]. \quad (2.19)$$

This equation can be simplified in two cases: a stationary distribution, i.e., $P(\phi, t) = P_s(\phi)$ independent of t , and a time-periodic distribution. In the first case,

$$V(t) = e^{L(P_s)t}, \quad (2.20)$$

and the stationary distribution is stable if all the eigenvalues of L have negative real parts, except for one eigenvalue which is equal to 0. This eigenvalue is associated with the unphysical perturbation $\delta P(\phi, t) \propto P_s$, which does not obey the normalization condition (2.8). The second case is when the distribution function is periodic in time with a period T_p . It is unstable if the operator $V(T_p)$ has eigenvalues whose absolute values are greater than 1.

C. Classification of the asymptotic behavior

At long times the system approaches a limiting trajectory. The limiting trajectory can be an attractor, i.e., stable to small perturbations. However, in our model there are cases where the limiting trajectory is not an attractor, but is marginal to some fluctuations.

The possible asymptotic behaviors of the system at large time can be classified according to the temporal and spatial properties of the various limiting trajectories, approached by the system at large time. The distribution function of the oscillators in the trajectories can be continuous or contain a sum of δ functions in ϕ . Analyzing the limit trajectories is the main goal of this work.

The possible limiting trajectories that are found in this system are the following.

1. Fixed point

Fixed points ϕ_0 satisfy $\dot{\phi} = 0$ for $\phi = \phi_0$. In general, many fixed points can exist. For those which are locally stable, all the eigenvalues of the matrix $M(\phi_0)$ are negative. The simplest attracting FP's are spatially homogeneous fixed points (HFP's), i.e., $\phi_{0i} = \phi_0$. The phase ϕ_0 is a solution of the equation

$$\omega + f(\phi_0) - g(\phi_0) = 0. \quad (2.21)$$

In this case the stability matrix M has one eigenvector that corresponds to a spatial homogeneous fluctuation, i.e., $\delta\phi_i = \delta\phi$, and the corresponding eigenvalue μ_1 is

$$\mu_1 = \frac{\partial f}{\partial \phi}(\phi_0) - \frac{\partial g}{\partial \phi}(\phi_0). \quad (2.22)$$

The other eigenvectors correspond to inhomogeneous fluctuations, i.e., $\sum_{i=1}^N \delta\phi_i = 0$. Their common eigenvalue μ_2 ,

$$\mu_2 = \frac{\partial f}{\partial \phi}(\phi_0), \quad (2.23)$$

has $(N-1)$ -fold degeneracy. The HFP is stable if μ_1 and μ_2 are negative. The stability analysis of inhomogeneous FP's is more complicated. However, in the regimes that were investigated in this work, the inhomogeneous FP's are not stable.

2. Limit cycles

In this limit trajectory the system moves periodically with time period T_p . There are special important kinds of periodic attractors.

a. Homogeneous limit cycle [$\phi_i(t) = \phi(t)$]. All the oscillators are coherent in phase and move together according to

$$\dot{\phi}_i = \omega \quad \forall_i, \quad \dot{\phi} = \omega + f(\phi) - g(\phi). \quad (2.24)$$

Note that for given f and g , the homogeneous limit cycle (HLC) and HFP do not coexist. In Appendix A it is shown, using Eq. (2.16), that the stability condition of the HLC, computed by integrating the nonuniform fluctuations along one period T_p of the trajectory, leads to

$$I_1 \equiv \int_0^{T_p} dt \frac{\partial f(\phi(t))}{d\phi} \\ = \int_0^{2\pi} d\phi \frac{\partial f(\phi)}{\partial \phi} \frac{1}{\omega + f(\phi) - g(\phi)} < 0. \quad (2.25)$$

b. Cluster states. The system breaks into N_c clusters. Within each cluster the phases of the oscillators are the same, but the phases between different clusters are functions of time. A state is termed a cluster state if N_c remains finite as $N \rightarrow \infty$, and it is inhomogeneous if $N_c > 1$. Thus the number of oscillators in each cluster is macroscopic. In the cluster state the distribution function is a sum of N_c δ functions, represented by their phases Φ_k . These phases evolve according to

$$\dot{\Phi}_k = \omega + f(\Phi_k) - \sum_{j=1}^{N_c} \epsilon_j g(\Phi_j), \quad k=1, \dots, N_c, \quad (2.26)$$

where $\epsilon_j N$ is the number of oscillators in the j th cluster and

$$\sum_{j=1}^{N_c} \epsilon_j = 1. \quad (2.27)$$

For stability analysis two kinds of fluctuations should be taken into account. There are fluctuations that keep the cluster state, but perturb the coordinates Φ_k of the clusters. The stability of these fluctuations is investigated by

perturbing the system of N_c equations (2.26). In addition, there are fluctuations that break the clusters. In Appendix A it is shown that the stability conditions associated with these nonuniform fluctuations are

$$I_k \equiv \int_0^{T_p} dt \frac{\partial f(\Phi_k(t))}{\partial \Phi_k} < 0, \quad k=1, \dots, N_c. \quad (2.28)$$

Note that the HLC is a degenerate case of this limiting trajectory with $N_c = 1$.

c. Stationary distribution. In this state the phases of the oscillators are smoothly distributed over $[0, 2\pi]$; i.e., there are no macroscopic clusters, and the continuous distribution is constant in time. From Eq. (2.5) one observes that the general form of such a stationary distribution (SD) is

$$P_s(\phi) = \frac{\nu}{\bar{\omega} + f(\phi)}, \quad (2.29)$$

where ν is determined by the normalization condition (2.8) and $\bar{\omega}$ is determined self-consistently from the equation

$$\bar{\omega} = \omega - \int_0^{2\pi} d\phi \frac{\nu g(\phi)}{\bar{\omega} + f(\phi)}. \quad (2.30)$$

The equation of motion of each oscillator is

$$\dot{\phi}_i = \bar{\omega} + f(\phi_i). \quad (2.31)$$

Thus all the oscillators move periodically with the same frequency. Generally, the phase difference between two oscillators changes with time. The number of solutions of Eq. (2.30) and the stability of the corresponding SD depend on the functions f and g .

Using the language of "currents," it is seen from Eqs. (2.10) and (2.11) that the particles' current $J(\phi, t)$ in the SD state for any point on the circle does not depend on space and time: $J(\phi, t) = J$. This is the condition for a *steady state*.

d. Other periodic continuous distributions. There are additional limit trajectories whose distribution functions are continuous in ϕ and periodic in t . The oscillators are periodic in t with the same period.

3. Nonperiodic trajectory

Nonperiodic behavior is observed in a small regime in the parameter space that defines the functions f and g (see Secs. III B and III C). The nonperiodic limit trajectories are either quasiperiodic or aperiodic, but this remains to be determined conclusively.

4. Quasiperiodic trajectory

In a special case (see Sec. III B), quasiperiodic limit trajectories have also been found.

It is convenient to use global order parameters in order to characterize the dynamical behavior of the system. Possible order parameters are the coefficients of the Fourier series of the distribution function. We use mainly the first Fourier component Z , which is defined as

$$Z(t) \equiv \frac{1}{N} \sum_{i=1}^N e^{i\phi_i(t)} = \int_0^{2\pi} d\phi P(\phi, t) e^{i\phi}. \quad (2.32)$$

In the cases of FP and SD, Z converges to a point in the complex plane. Generally, when the distribution depends on time, Z is also time dependent. In the case of the HLC, the limit trajectory of Z in the complex plane is a unit circle.

D. Numerical methods

In most cases the study of the present system requires the use of numerical methods. Two types of numerical studies have been used in this work: simulations of networks with N oscillators by numerical integration of the system of Eq. (2.1) and numerical solution of the continuity equation (2.5). Simulations of Eq. (2.1) have been performed by integrating the equations of motion with a fourth-order Runge-Kutta algorithm. The time step Δt was chosen to be 0.01 for $\omega=1$ [6]. We have checked that decreasing the time step does not significantly affect the results. Networks of 100–10 000 oscillators were considered, but it was verified that in general reliable results are obtained already with a network of 100 oscillators. The initial conditions of the oscillators were chosen randomly according to three possible initial distributions of the oscillators phases: (1) uniform distribution, (2) sharp Gaussian distribution with standard deviation 0.05, and (3) distribution with several (two to five) sharp Gaussian peaks, all of them with a standard deviation 0.05.

We have also solved numerically the continuity equation. Besides reconfirming the results of the simulation, this numerical method helps us to understand what happens to the system in the limit $N \rightarrow \infty$ and eliminates the influence of finite-size effects. Equation (2.5) was solved in Fourier space [10]. The infinite set of ordinary differential equations for the Fourier components of the distribution was truncated. We obtained a finite number of equations and solved them by using a fourth-order Runge-Kutta method [10]. The validity of the truncation was checked by comparing the results obtained by taking into account different number of Fourier components. It is clear that such a truncation is not justified when the distribution function has one or more δ -function peaks, as in the case of the HFP or cluster LC's. However, when the limiting distribution is smooth in ϕ , this method gives reliable results that are in good agreement with the simulations.

III. SOME SPECIAL CASES OF f AND g

$$\begin{aligned} \text{A. Case I: } f(\phi) &= A \sin(\phi), \\ g(\phi) &= \sigma \sin(\phi + \alpha) \end{aligned}$$

As a first case, we consider the situation where both f and g contain only the $n=1$ Fourier component:

$$f(\phi) = A \sin(\phi), \quad g(\phi) = \sigma \sin(\phi + \alpha). \quad (3.1)$$

By changing the normalizations one can always redefine the problem such that

$$\omega > 0, \quad A > 0, \quad 0 \leq \alpha < \pi. \quad (3.2)$$

In this section we will discuss the case $\alpha \neq 0$. The case $\alpha = 0$ is special and will be discussed in Sec. III B.

For all values of the parameters, there exists either a homogeneous FP (HFP) or a homogeneous LC (HLC). Equation (2.21) for the HFP ($\phi_i = \phi_0$) becomes

$$\sin(\phi_0 - \tilde{\phi}) = -\frac{\omega}{\tilde{A}}, \quad (3.3)$$

where

$$\tilde{A} = (A^2 - 2\sigma A \cos \alpha + \sigma^2)^{1/2}, \quad (3.4)$$

$$\tilde{\phi} = \arctan \frac{\sigma \sin \alpha}{A - \sigma \cos \alpha}. \quad (3.5)$$

A homogeneous FP exists outside the ellipse $A^2 - 2A\sigma \cos \alpha + \sigma^2 = \omega^2$. Equation (3.3) has two solutions, but only one of them is stable to uniform fluctuations. Using Eqs. (2.22) and (2.23), one can show that stability to both uniform and nonuniform fluctuations occurs if and only if

$$\sigma \cos \alpha < A - \omega \quad (3.6)$$

or if

$$\sigma \cos \alpha < A + \omega \quad \text{and} \quad \sigma < 0. \quad (3.7)$$

In the domain where this FP does not exist, a homogeneous LC exists. The stability condition [Eq. (2.25)] is found to be

$$\begin{aligned} I_1 &= \int_0^{2\pi} d\phi \frac{A \cos \phi}{\omega + \tilde{A} \sin(\phi - \tilde{\phi})} \\ &= \frac{2\pi A [\omega - (\omega^2 - \tilde{A}^2)^{1/2}]}{\tilde{A}^2 (\omega^2 - \tilde{A}^2)^{1/2}} \sigma \sin \alpha < 0. \end{aligned} \quad (3.8)$$

Thus the stability condition is

$$\sigma < 0. \quad (3.9)$$

Besides the FP and HLC, the stationary distribution state may also exist. This distribution (2.29) has the form

$$P_s(\phi) = \frac{\nu}{\tilde{\omega} + A \sin(\phi)}. \quad (3.10)$$

Using Eqs. (3.10), (2.30), and (2.8), one obtains

$$\nu = \frac{1}{2\pi} (\tilde{\omega}^2 - A^2)^{1/2}, \quad (3.11)$$

$$\tilde{\omega} = \omega + (\tilde{\omega} - 2\pi\nu) \frac{\sigma}{A} \cos \alpha. \quad (3.12)$$

Equations (3.11) and (3.12) have a solution with $\tilde{\omega} > 0$ if

$$\sigma \cos \alpha > A - \omega \quad \text{and} \quad \sigma \cos \alpha > 0 \quad (3.13)$$

or

$$\frac{A^2 - \omega^2}{2A} < \sigma \cos \alpha < 0. \quad (3.14)$$

Note that $\tilde{\omega}$ has to obey the inequality $\omega - |\sigma \cos \alpha| \leq \tilde{\omega} \leq \omega + |\sigma \cos \alpha|$ [see Eq. (2.30)]. From the stability analysis of the SD, reported in Appendix B, it is

found that the SD with a positive $\tilde{\omega}$ is marginal in the regime

$$\sigma > 0. \quad (3.15)$$

In this regime all the eigenvalues of the stability operator L are pure imaginary except two complex conjugate eigenvalues that have negative real part [as shown in Fig. 7(a)]. Besides this SD, there exists another SD with negative $\tilde{\omega}$ if $\sigma \cos\alpha > A + \omega$. However, this SD is always unstable. The regime where a *marginal* SD exists is termed in the following as the *marginal regime*. The different regimes are displayed in Fig. 1(a) for $\alpha = \pi/4$ and in Fig. 1(b) for $\alpha = \pi/2$.

There are also cluster states for all arbitrary $N_c > 1$. For each N_c there is a regime of ϵ_j for which a solution exists. It was found that the N_c clusters (with $N_c > 1$) exist only in the marginal regime. These cluster states were found numerically to be stable to intercluster fluctuations. The stability of a cluster state to intracluster fluctuations was found by calculating the N_c integrals [Eq. (2.28)], which become

$$I_k = \int_0^{T_p} dt \cos[\Phi_k(t)], \quad k=1, \dots, N_c. \quad (3.16)$$

The trajectory cannot be expressed in an analytical closed form, and we are only able to compute this integral nu-

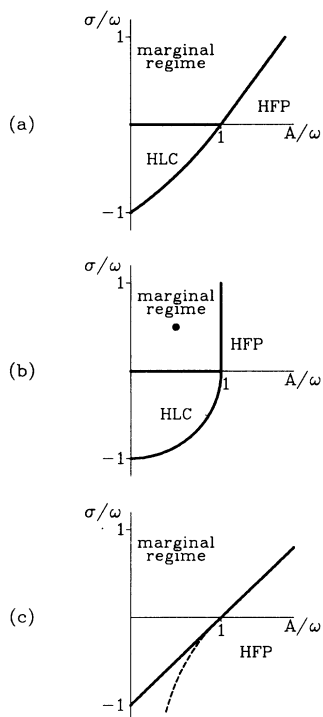


FIG. 1. Phase diagram of the model defined in Eq. (2.1), where $\omega=1$, $f(\phi) = A \sin(\phi)$, and $g(\phi) = \sigma \sin(\phi + \alpha)$. In the regime denoted by “HFP,” the HFP exists and is stable. The HLC exists and is stable in the regime denoted by “HLC.” In the marginal regime the SD exists and is marginal. (a) $\alpha = \pi/4$. (b) $\alpha = \pi/2$. The solid circle represents the parameters chosen in Fig. 4. (c) $\alpha = 0$. On the left side of the dashed curve, both a stable HFP and a marginal SD exist.

merically for particular values of the parameters A , σ , and α in the marginal regime. In all the cases we have considered, we have shown that the N_c clusters are marginal; i.e., all I_k vanish, as long as there is no cluster that contains more than half of the oscillators, i.e., $\epsilon_k < \frac{1}{2}$ for all k . Otherwise, one I_k is positive and the cluster state is unstable. For example, the two-cluster state is marginal; i.e., the integrals I_1 and I_2 are zero, if the number of oscillators in each cluster is equal: $\epsilon_1 = \epsilon_2$.

The analysis that was presented here is linear. Using it, we can neither find the basins of attractions of the limit trajectories nor find what happens to the system when we begin with general initial conditions, especially in the marginal regime. In order to investigate these questions, numerical simulations of Eq. (2.1) were performed. The simulation results are characterized conveniently by measuring the order parameter Z [Eq. (2.32)]. It is found that in the regimes where the HFP or HLC were stable, they were global attractors and the oscillators *always* converged to them.

The situation is more interesting in the marginal regime. The main result of the simulations in this regime is that for most initial conditions the system does not converge to one of the above-mentioned limit trajectories. Instead, the attracting set consists of a manifold of inhomogeneous periodic trajectories. The limiting trajectory depends on the initial condition—different initial conditions usually lead to different trajectories. We can see that these trajectories are not attractors by letting the system converge to one of them. Then the values of the oscillators are changed by a small amount, and the dynamics is run again. It is seen [Fig. 2(a)] that the system converges to another trajectory, which is close to the original one, but does not coincide with it.

Usually, trajectories are characterized by continuous distribution functions, which are periodic in time. However, there can be also mixed states where some (but less than half) of the oscillators belong to a cluster and the others are distributed continuously. This can happen, for example, if the initial distribution has two peaks.

It was found numerically that, in every trajectory in the marginal regime,

$$\int_0^{T_p} dt \cos[\phi_i(t)] = 0, \quad \forall i. \quad (3.17)$$

However, we do not have any general proof for this result, except for the case of the SD.

The continuity equation (2.5) was also solved in this case. Starting from a uniform initial distribution function in the marginal regime (for instance, $A=0.5$, $\sigma=0.5$, $\alpha = \pi/4$), it was found that the stationary distribution is reached asymptotically at long times. However, for a general initial distribution, the solution of Eq. (2.5) leads to a distribution which evolves periodically in time, as shown in Fig. 2(b).

B. Case II: $f(\phi) = A \sin(\phi)$, $g(\phi) = \sigma \sin(\phi)$

This is a special case of the previous subsection with $\alpha=0$. The model with this choice of f and g has been used to describe a linear series array of Josephson junc-

tions, in which the load is purely resistive and the capacitance of the junction is neglected [11,12].

The existence and stability of the simple attractors are found using the formulas developed in the previous section. The HFP exists in the regime $|\sigma - A| > \omega$ and is stable if $\sigma < A - \omega$. The HLC exists in the regime $|\sigma - A| < \omega$, and its stability is marginal there. The SD with positive $\bar{\omega}$ exists if $\sigma > A - \omega$ and $\sigma > 0$ or if $(A^2 - \omega^2)/2A < \sigma < 0$. From Eqs. (B16) and (B20), it is seen that all the eigenvalues of the stability operator L of the SD are purely imaginary. Thus the SD is marginally stable *in all directions*. The region where the SD is marginally stable is again called the marginal regime. The N_c -cluster states are also marginal, both to intracluster and intercluster fluctuations. For fixed values of N_c and ϵ_k , $k = 1, \dots, N_c$, there is a continuum of limit trajectories in the space of the coordinates Φ_k of the clusters, which depend on the initial condition. This occurs also at $N=2$ and $\epsilon_1 = \epsilon_2 = 0.5$, as shown in [12]. The phase diagram for this case is represented in Fig. 1(c).

The system was simulated numerically for large N (100–1000) with initial conditions that are chosen ran-

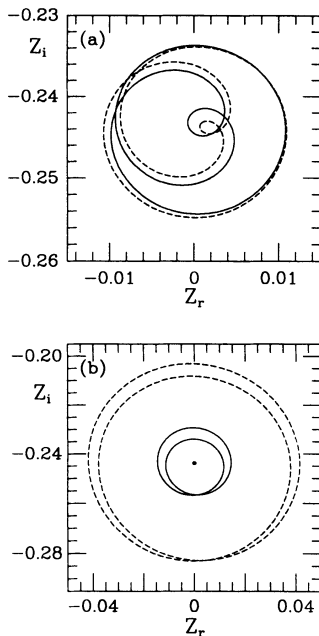


FIG. 2. Limiting trajectory of the order parameter Z (solid line) obtained from simulating Eq. (2.1) with $N=100$. The parameters $\omega=1$, $A=0.5$, $\sigma=0.5$, and $\alpha=\pi/4$ belong to the marginal regime [Fig. 1(a)]. The dashed line is the limiting trajectory that is obtained after changing all the phases by a random number taken from a distribution with 0.1 rad standard deviation. This trajectory is close to the first one, but they are not identical. (b) The limiting trajectories of Z obtained from the solution of the continuity equation (2.5) for three different initial distributions. The initial distribution is defined by its Fourier component a_n^0 . We chose $a_n^0=0$ for $n \geq 4$. Initial distribution with $a_1^0=0.2$, $a_2^0=0.2$, and $a_3^0=0.1$ leads to the outer cycle; initial distribution with $a_1^0=0.05$, $a_2^0=0.05$, and $a_3^0=0.05$ leads to the middle cycle; and initial distribution with $a_1^0=a_2^0=a_3^0=0$ leads to the stationary distribution represented by the solid circle.

domly from a uniform or sharp distribution (see Sec. IID). When the HFP was stable, it was found that the system converged to it for all the initial conditions that were checked. Thus the basin of attraction of the stable HFP for large N is very large. This should be compared to the situation for $N=2$, where there is a domain of coexistence of two types of limiting trajectory: a HFP and nonhomogeneous cycles [12].

The situation is more interesting when there is no stable HFP. The limiting trajectories of the system are either quasiperiodic, usually with two basic frequencies, or aperiodic. This is in contrast to the case $\alpha \neq 0$, where the limiting trajectories are periodic. As in the case of $\alpha=0$, the trajectories depend on the initial conditions—a small change in the initial condition causes a change in the limit trajectory. However, in the $\alpha=0$ case, even the qualitative behavior of the limit trajectory may depend on the initial conditions. As an example, we present the case of $A=0.5$ and $\sigma=1.0$. When the initial conditions are taken randomly from a uniform distribution of phases, the limiting trajectory is quasiperiodic with two basic frequencies, as is shown in Figs. 3(a)–3(c). The

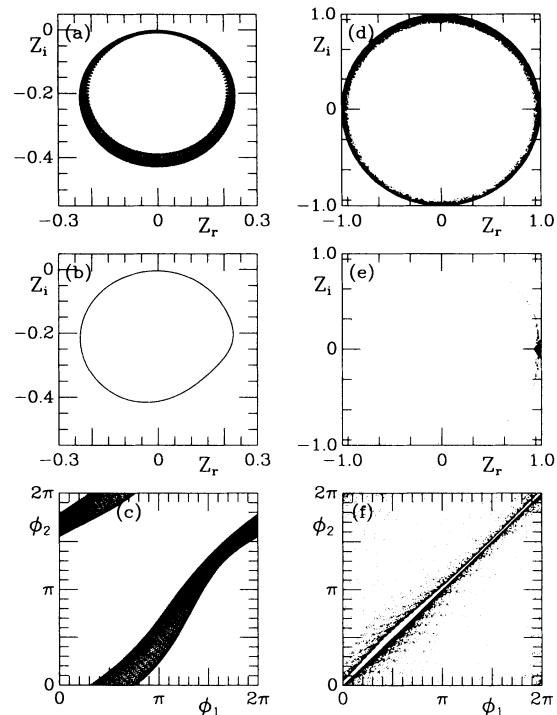


FIG. 3. Limit trajectory in the case $\omega=1$, $f(\phi)=0.5 \sin(\phi)$, and $g(\phi)=1.0 \sin(\phi+\alpha)$ obtained from simulating Eq. (2.1) with $N=100$. The system is in the marginal regime [Fig. 1(c)]. (a)–(c) The initial conditions are taken from uniform distribution. (a) The order parameter Z . (b) Poincaré section of the trajectory. It is obtained by plotting the value of Z every time when the phase ϕ_1 is zero. The Poincaré section is a close line, implying that the full trajectory is quasiperiodic with two basic frequencies. (c) Projection of the limit trajectory on the space of two oscillators ϕ_1 and ϕ_2 . (d)–(f) The initial conditions are taken from a Gaussian distribution with standard deviation 0.05. The motion is aperiodic. (d) The order parameter Z , (e) Poincaré section of the trajectory, and (f) projection of the limit trajectory on the space of two oscillators ϕ_1 and ϕ_2 .

Poincaré section of Z is a cycle [see Fig. 3(b)]. However, if the initial conditions are taken from a sharp distribution with 0.05 rad standard deviation, the limiting trajectory is aperiodic and probably chaotic, as appears in the analysis of the motion, performed using Fourier transform and Poincaré section. This case is presented in Figs. 3(d)–3(f).

This huge marginality in the case $\alpha=0$ may be related to the symmetry of the system (2.1) under the transformation $t \rightarrow -t$, $\phi \rightarrow \pi - \phi$ in the case of $f(\phi) = A \sin(\phi)$, $g(\phi) = \sigma \sin(\phi)$ [12]. This generalized time-reversal symmetry may be the origin of the conservative-type behavior of the oscillators that occurs at some parameters in (at least) part of the phase space [12]. However, it should be emphasized that marginality of the limit trajectories exists also in the case $\alpha \neq 0$, as observed in Sec. III A, although there is no obvious symmetry in that case.

C. Case III: Resolving the marginality: f with three harmonics

The marginality of limiting trajectories in the case $f(\phi) = A_1 \sin(\phi)$, $g(\phi) = \sigma_1 \sin(\phi + \alpha_1)$ is resolved if more Fourier components are added to the functions f and g . We have studied in detail the following coupled ordinary differential equation:

$$\dot{\phi}_i = \omega + \sum_{n=1}^3 A_n \sin(n\phi_i) - \frac{\sigma_1}{N} \sum_{j=1}^N \sin(\phi_j + \alpha), \quad i = 1, \dots, N. \quad (3.18)$$

The model (3.18) with $A_2, A_3 \neq 0$ does not exhibit a marginal regime, and the system always converges to attractors. In the following we focus our attention on the values of A_1 , σ_1 , and α such that, if the higher harmonics vanish, the system would be in the marginal regime. When the amplitudes of the higher harmonics are small, the system converges to one of the following attractors: (1) the cluster state with N_c macroscopic clusters, (2) a periodic state with a stationary distribution, or (3) a non-periodic state with a continuous distribution. The phase diagram of the model is represented in Fig. 4, where the attraction regimes of these attractors are shown. In this phase diagram we have included only cluster states with $N_c \leq 3$.

In general, the cluster state is not unique even for a given N_c . There may be trajectories with different distributions of oscillators between the clusters, i.e., with different ϵ_j of Eq. (2.26). The N_c clusters are stable to intracluster fluctuations if the largest value of all the integrals I_k is negative [Eq. (2.28)], and these integrals depend on the fraction of oscillators in each cluster. It was found in all the cases studied that the maximal integral is smallest when the number of oscillators in each cluster is equal, i.e., $\epsilon_i = \epsilon_j$ for all i, j [see Eq. (2.26)]. In the case of $N_c = 2$, the two stability integrals are shown in Fig. 5 vs $|\epsilon_1 - \epsilon_2|$ for typical values of the parameters. It is seen that the large stability integral increases with $|\epsilon_1 - \epsilon_2|$ until it become positive, signaling the instability of the two-cluster state for larger values of $|\epsilon_1 - \epsilon_2|$. Similar results were obtained for coupled maps [13,14]. We have used

the fact that the N_c -cluster state with equal number of oscillators has the most stable cluster trajectories, to find the borders of the regions where the two- and three-cluster states are stable. Near the border of such a region, the stability region in the ϵ space shrinks. On the border the solution with equal ϵ_k is marginal and all the others are unstable.

The stability regions of the two- and three-cluster states are shown in Fig. 4. There are regions where only the two- or three-cluster state is stable. There is a region when both states are stable, and there is a region where neither one is stable. Stable cluster states with $N_c = 4, 5, \dots$ were also found. For example, in most of the regime where the three-cluster state is stable and the two-cluster state is unstable, there is a stable four-cluster state. Numerical simulations of the full system [Eq. (2.1)] reveal that when the cluster states are stable, the system converges to them. The system tends to converge to a cluster state with a *minimal* number of clusters if the initial conditions are taken from a uniform or a sharp distri-

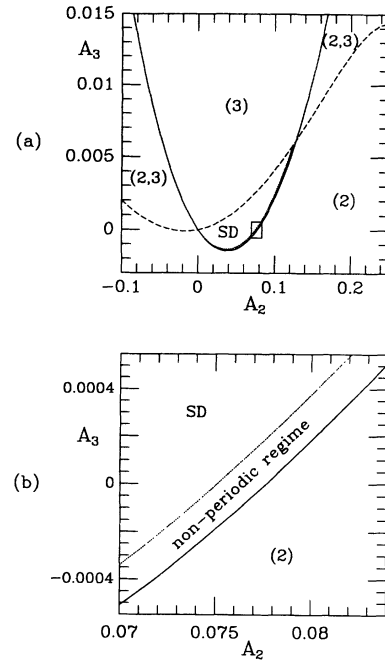


FIG. 4. Phase diagram of the model in the case $\omega=1$, $f(\phi) = \sum_{n=1}^3 A_n \sin(n\phi)$, $A_1=0.5$, and $g(\phi) = 0.5 \sin(\phi + \pi/2)$. Note that with $A_2 = A_3 = 0$, the parameters belong to the marginal regime as seen in Fig. 1(b). The solid line represents the border of stability of the two-cluster states, the dashed line represents the border of stability of the three-cluster states, and the dotted line represents the border of stability of the second mode of L , the stability operator of the SD. Numbers such as (2,3) indicate the stable cluster states in each region; the region where the stationary distribution is stable is labeled by SD. There is a nonperiodic regime between the solid and dotted lines. Stable cluster states with 4, 5, ... clusters may also exist in parts of the regime of this figure where stable two- or three-cluster states exist. However, the borders of existence of cluster states with $N_c \geq 4$ are not presented. (b) shows an expanded view of the square marked in (a).

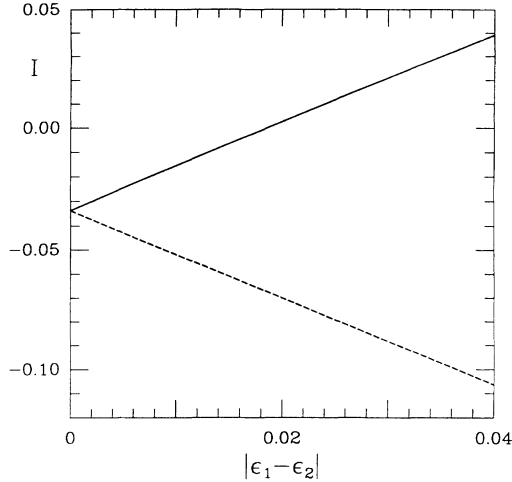


FIG. 5. Stability integrals I_1 (solid line) and I_2 (dashed line) of the two-cluster states vs $|\epsilon_1 - \epsilon_2|$. $A_1=0.5$, $A_2=0.2$, $\psi_2=0$, $\sigma_1=0.5$, $\alpha_1=\pi/2$, and all the other A_n and σ_n are zero. When one integral is positive, the corresponding cluster is unstable to nonuniform fluctuations. Here the two-cluster states are stable if $|\epsilon_1 - \epsilon_2| < 0.02$.

bution with one peak. If a cluster state with higher N_c is stable, the system can converge to it if the initial conditions are taken from a distribution with N_c peaks. This fact indicates that the basin of attraction of the cluster state with the minimal N_c is much larger than the basin of attraction of the cluster states with bigger N_c .

The stability of the state with a stationary distribution (SD) is numerically studied by calculating the eigenvalues λ_n of the operator L [Eq. (2.18)]. The eigenvalues can be ordered according to their imaginary parts. The number of maxima of both the real and imaginary parts of the eigenvector as a function of ϕ is equal to n . For all the cases that were studied, it was found that if both $\text{Re}\lambda_2$ and $\text{Re}\lambda_3$ are negative, the real part of all the other eigenvalues is negative too, and the SD is stable. In Fig. 4 it is seen that the regime in A_2 - A_3 , where the SD is stable, is inside the regime where the two- and three-cluster states are not stable. An N_c -cluster state is stable only if the N_c mode of the SD is not stable.

From the phase diagram (Fig. 4), it is apparent that there is a small region between the line where $\lambda_2=0$ and the line of stability of the two-cluster state. In this area neither the SD nor the cluster states are stable. Numerical simulations of the system in this regime reveal that the trajectory of each rotator, as well as the distribution as a whole, are nonperiodic in time. This is shown in Fig. 6(a) by plotting points of the trajectory in the Z plane. The distribution of oscillator phases is represented in Fig. 6(b) for several times. In this case the probability distribution has two peaks, but the attraction among the oscillators at those peaks is not strong enough to generate full clustering. The Fourier transform of $Z(t)$ or $\phi_i(t)$ exhibits two basic frequencies, indicating a quasiperiodic state. However, the Poincaré section is not a line, and so the motion may have another, very slow, component. There-

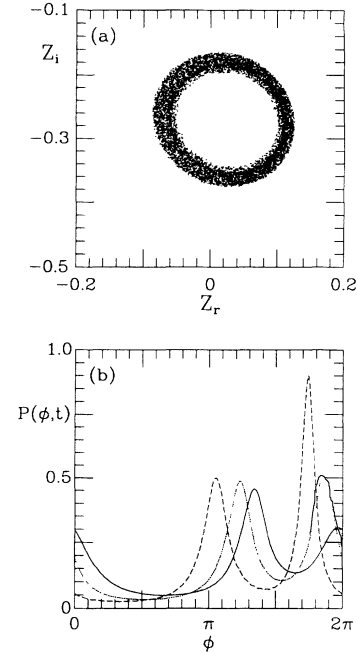


FIG. 6. System is in the nonperiodic regime for $\omega=1$, $f(\phi)=0.5 \sin(\phi)+0.077 \sin(2\phi)$, and $g(\phi)=0.5 \sin(\phi+\pi/2)$. (a) The limit trajectory of the order parameter Z for these values of the parameters and (b) the distribution function in the nonperiodic regime for several times: $t=1.5 \times 10^5$ (solid line), $t=1.8 \times 10^5$ (dotted line), and $t=2.1 \times 10^5$ (dashed line).

fore, it is possible that it is aperiodic and even chaotic. Since the dynamics in this regime is very slow, more simulations for longer times are needed for better understanding of the temporal structure of this attractor.

We have investigated also, but in less detail, more general cases. When more Fourier components A_4, A_5, \dots were added to f , but g had only the first harmonic, all the qualitative results remained valid. When more Fourier components are added also to g , a cluster state with $N_c > 3$ clusters can have a large basin of attraction and the system can converge to it, even if the initial conditions are taken from the uniform or sharp distribution.

IV. DYNAMICS WITH STOCHASTIC NOISE

A. Model with noise

In many real physical and biological systems, the dynamics is not purely deterministic, but is also affected by some stochastic noise. Here the effect of white noise on the behavior of the system of oscillators is investigated. The equations of motion in the presence of noise are

$$\dot{\phi}_i = \omega + f(\phi_i) - \frac{1}{N} \sum_{j=1}^N g(\phi_j) + \xi_i(t),$$

$$i = 1, \dots, N \quad (4.1)$$

where the “temperaturelike” noise $\xi_i(t)$ is Gaussian and uncorrelated:

$$\langle \xi_i(t) \rangle = 0, \quad (4.2)$$

$$\langle \xi_i(t)\xi_j(t') \rangle = 2T\delta_{i,j}\delta(t-t'). \quad (4.3)$$

In contrast to the case $T=0$, numerical simulation of Eq. (4.1) is not an efficient method, because one has to average over many realizations of the noise $\xi_i(t)$ in order to obtain a good statistical average. In addition, N must be large enough. Otherwise, the thermal fluctuations will cause all ensemble averages to be constant in time and will destroy ergodicity breaking phases that may exist in the $N \rightarrow \infty$ limit. Instead of solving Eq. (4.1) directly, it is more efficient to study the average single-phase distribution function. This function $P(\phi, t)$ is defined as

$$P(\phi, t) = \left\langle \lim_{N \rightarrow \infty} \frac{1}{N} \sum_{i=1}^N \delta(\phi - \phi_i) \right\rangle, \quad (4.4)$$

where $\langle \rangle$ means averaging over the noise. This function

$$\begin{aligned} \dot{a}_n = & (in\omega - n^2T)a_n + \frac{n}{2} \sum_{m=1}^{\infty} A_m [(a_{n+m} - a_{n-m})\cos\psi_m + i(a_{n+m} + a_{n-m})\sin\psi_m] \\ & - \frac{n}{2} a_n \sum_{m=1}^{\infty} \sigma_m [(a_m - a_{-m})\cos\alpha_m + i(a_m + a_{-m})\sin\alpha_m]. \end{aligned} \quad (4.7)$$

From the normalization condition, $a_0=1$. The infinite set of equations was truncated at some value of n, n_0 , substituting $a_n=0$ for $n > n_0$. This leads to a finite set of equations which was solved numerically using a fourth-order Runge-Kutta method [10]. The Fourier coefficients a_n decay sufficiently fast with n when $T > 0$ because $P(\phi, t)$ is smooth in ϕ . Therefore the truncation method is a good approximation. The validity of the truncation was checked by comparing the results obtained for different values of n_0 .

The stationary distribution (SD) is given by the solution of the differential equation

$$\{[\bar{\omega} + f(\phi)]P_s(\phi)\} - T \frac{\partial P_s(\phi)}{\partial \phi} = \nu, \quad (4.8)$$

with the conditions (2.7) and (2.9). The quantities ν and $\bar{\omega}$ are calculated from Eq. (2.6) and the normalization condition (2.8). The methods for evaluating $\bar{\omega}$ and ν explicitly and analyzing the stability are of the SD described in Appendix C.

B. Effects of noise on the long-time behavior

When N is finite, the system is ergodic, and all ensemble-averaged quantities are constant in time. In the limit $N \rightarrow \infty$, we still expect the system to be ergodic at high noise levels. In the ergodic phase, the system will converge at long times to the SD state. However, this ergodicity may be broken at low noise level and there may be a phase transition from a stationary phase to a time-dependent phase.

For all the parameter regimes, it was found that the noise tends to stabilize the SD, i.e., decreases the real part of the eigenvalues of the stability operator L [Eq. (C3)]. At low levels of noise, the behavior of the system depends on the nature of its state at $T=0$. Here we discuss our

satisfies the Fokker-Planck equation [15]

$$\begin{aligned} \frac{\partial}{\partial t} P(\phi, t) + \frac{\partial}{\partial \phi} \{[\bar{\omega}(t) + f(\phi)]P(\phi, t)\} \\ = T \frac{\partial^2 P(\phi, t)}{\partial \phi^2}, \end{aligned} \quad (4.5)$$

where $\bar{\omega}(t)$ is defined in Eq. (2.6). The distribution function should obey conditions (2.7)–(2.9). The Fokker-Planck equation (4.5) was solved in Fourier space [10]. Substituting

$$P(\phi, t) = \frac{1}{2\pi} \sum_{n=-\infty}^{\infty} a_n(t) e^{-in\phi}, \quad (4.6)$$

in Eq. (4.5), and using Eq. (2.2) yields an infinite set of coupled differential equations:

results for the main three regimes. These results are based on the numerical solution of Eq. (4.5) and on the stability analysis for the SD.

1. SD regime

In the regime where the SD state is stable and attracting at $T=0$, it continues to be the global attractor also at $T > 0$.

2. Marginal regime

In the regime where the SD is marginal at $T=0$, there is a phase transition at $T_c=0$ and any finite noise stabilizes the SD state, which becomes the global attractor.

In Fig. 7(a) the spectrum of the stability operator L at finite T [Eq. (C3)] is exhibited for three values of T : $T=0$, 1×10^{-4} , and 3×10^{-4} . It is seen that all the eigenvalues $\lambda_{\pm n}$ with $n \geq 2$, which are marginal at $T=0$, have a negative real part at $T > 0$. The real part of the two eigenvalues $\lambda_{\pm 1}$ remains negative when $T > 0$. This suggests that a small amount of noise stabilizes the SD in the marginal regime. This is corroborated by the results of Fig. 7(b), where the real parts of some of the eigenvalues are shown as a function of T . It is seen that $\text{Re}(\lambda_n)$ grows linearly with T . Numerically, we find that, for small T ,

$$\frac{\text{Re}\lambda_n}{n^2T} = \text{const}, \quad n \geq 2. \quad (4.9)$$

3. Cluster-state regime

In the cluster-state regime, where the SD is unstable at $T=0$, it is unstable also at $T < T_c$, where $T_c > 0$. There is a phase transition at the critical noise level T_c , above which the SD is the global attractor. Below T_c the distri-

bution $P(\phi, t)$ is periodic in time. The cluster structure is smeared because of the noise. Hence the peaks in ϕ dependence of $P(\phi, t)$ acquire finite width. An example is shown in Fig. 8(a).

The trajectories of the order parameter Z for some values of T in this regime are represented in Fig. 8(b). At low T the radius of the limit cycle of Z remains finite. It shrinks to zero as $T \rightarrow T_c$. The magnitude of the time dependence of Z is measured by the parameter Z_{rms} , which measures the rms average of the distance between a point on the cycle and its center:

$$Z_{\text{rms}} \equiv \left[\frac{1}{T_p} \int_0^{T_p} dt |Z(t) - \bar{Z}|^2 \right]^{1/2}, \quad (4.10)$$

where

$$\bar{Z} = \frac{1}{T_p} \int_0^{T_p} dt Z(t). \quad (4.11)$$

The dependence of Z_{rms} on T is presented in Fig. 8(c). The results are analogous to a second-order phase transition in equilibrium statistical mechanics. The order parameter Z_{rms} vanishes continuously when T increases toward T_c . Its vanishing with T near T_c from below is consistent with a critical exponent $\frac{1}{2}$, i.e.,

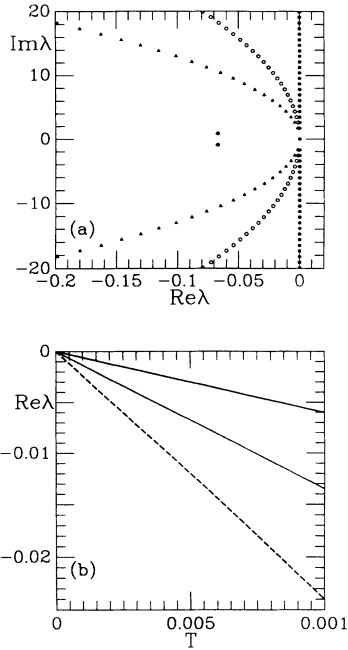


FIG. 7. Spectrum of the stability operator L for different values of the noise T . For $T=0$ (solid circles) the system is in the marginal regime. All the eigenvalues of L have zero real parts, except two eigenvalues $\lambda_{\pm 1}$ whose real part is negative. For $T=1 \times 10^4$ (open circles) and $T=3 \times 10^4$ (triangle), the real part of the eigenvalues λ_n with $n \geq 2$ is negative. The change in the eigenvalues $\lambda_{\pm 1}$ is small and is not seen in the figure. The parameters are $A_1=0.5$, $\sigma_1=0.5$, and $\alpha_1=\pi/2$. (b) The T dependence of the real part of eigenvalues λ_2 (solid line), λ_3 (dotted line), and λ_4 (dashed line) of the stability operator L .

$$Z_{\text{rms}}(T) \propto (T_c - T)^{1/2}. \quad (4.12)$$

Note that this transition is similar to a Hopf bifurcation [17] in that the frequency of the oscillators remains finite as $T \rightarrow T_c$.

V. DISCUSSION

The phase model studied here is a generalization of the model proposed and studied in the context of linear arrays of Josephson junctions [11], where the local non-linear function was restricted to $f(\phi) = A \sin(\phi)$ and the interaction term to $g(\phi) = \sigma \sin(\phi)$. In this case there is a regime where there is no attractor, but rather a *continuum* of marginal limit trajectories. Studying this case, it has been argued [12] that the nonattractive behavior results from the existence of a *generalized time-reversal symmetry* $\phi \rightarrow \pi - \phi$ and $t \rightarrow -t$, which leads to a conser-

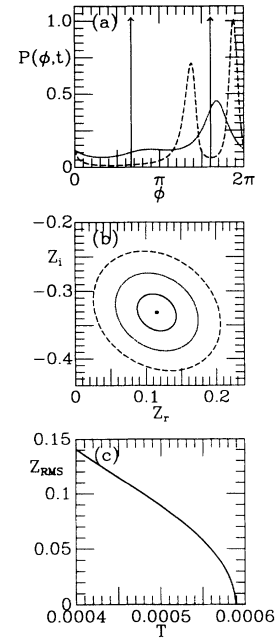


FIG. 8. Behavior of the oscillator system when noise is added. The system is in the two-clusters regime when $T=0$. $A_1=0.5$, $A_2=0.3$, $\psi_2=0$, $\sigma_1=0.5$, $\alpha_1=\pi/2$, and all the other A_n and σ_n are zero. The critical temperature is $T_c=5.885 \times 10^{-4}$. Above the critical temperature, the SD is stable. Below it the distribution function is periodic in time. (a) The distribution function $P(\phi, t)$ for fixed t and several values of T . At $T=0$ the system consists of two clusters, represented by two δ peaks. Below T_c two peaks with finite width that evolve periodically in time are found. The distribution function at $T=2 \times 10^{-4}$ ($< T_c$) is represented by the dashed line. Above T_c the distribution function is stationary. It is represented for $T=1.0 \times 10^{-3}$ ($> T_c$) by the dotted line. (b) The limiting trajectory of the order parameter Z for some values of T : $T=5 \times 10^{-4}$ (dashed line), $T=5.5 \times 10^{-4}$ (dotted line), $T=5.8 \times 10^{-4}$ (solid line), and $T=6 \times 10^{-4}$ (solid circle). (c) The order parameter Z_{rms} [see Eq. (4.10)] vs T . The system undergoes a second-order transition from a periodic state to a steady state.

vative behavior, at least in part of phase space. However, we have found that the marginality exists also in the case of $f(\phi) = A \sin(\phi)$ and $g(\phi) = \sigma \sin(\phi + \alpha)$ with $\alpha \neq 0$, where there is no such symmetry. It would be interesting to understand the origin of this marginality in the general- α case.

For functions f and g which include higher harmonics, the system converges to well-separated attractors. The differential equations of all the oscillators in our model are the same, and the coupling has an infinite range. Therefore, naively, one would expect to find either a completely homogeneous state (e.g., a homogeneous fixed point or a homogeneous limit cycle) or a completely inhomogeneous state, i.e., a state with a stationary distribution. Such attractors have been actually found. A main result of our study is that the system often converges to *cluster states*, i.e., to partially homogeneous states. The appearance of cluster states represents a spontaneous breaking of the spatial symmetry of the system.

Each attractor in the cluster-state regime is, of course, highly degenerate, as the grouping of the oscillators into clusters is arbitrary. This degeneracy can be broken by external inputs whose spatial structure has a significant overlap with a particular clustering pattern. Thus our system can recognize and amplify spatial structures in external patterns. This may give a new insight about the possible functional relevance of synchronized oscillatory neural networks [3,4].

Adding noise to the system causes the smearing of the cluster states. Below a critical value of noise, the state of the system is nonergodic in the limit $N \rightarrow \infty$. This is manifested by the single-phase distribution function, which is periodic in time, despite the presence of stochastic noise. It has some peaks with finite width in its ϕ dependence. At a critical noise level, a phase transition occurs and the distribution function is constant in time. In the marginal regime, any finite noise causes the stationary distribution to be the global attractor. Stabilization of the steady-state attractor by stochastic noise is shown also in [16], in the context of Kuramoto's model [1].

In both the state with stationary phase distribution and the cluster states, the phases are periodic in time. In a narrow regime of parameters, there exists a nonperiodic attractor, characterized by a continuous distribution of phases that display complex time dependence (see Fig. 6). A more systematic analysis and more time-consuming simulations are needed to understand the temporal structure of this attractor.

It is interesting to compare our model to other models with infinite-range interactions. Kaneko [13] has studied chaos in systems of maps coupled by uniform infinite-

range interaction. In these systems the appearance of chaos is not surprising since the local maps are already chaotic. Perhaps more relevant to this work are the chaotic phases found in neural networks [18] and coupled Ginzburg-Landau oscillators [19], as in both cases the local elements are linear elements or limit cycles. Nevertheless, these models differ from the present one in that they are not spatially uniform. In the case of neural networks, the couplings were random; in the Ginzburg-Landau model, the local frequencies are random. Thus our model is unique in that it represents a global coupling between simple oscillators in a uniform system. It is therefore surprising to find nonperiodic behavior in such a system.

ACKNOWLEDGMENTS

We thank J. P. Eckmann, P. C. Hohenberg, S. D. Fisher, and Z. Olami for useful discussions, and S. Strogatz for a helpful correspondence. This work was supported, in part, by the Fund for Basic Research administered by the Israeli Academy of Arts and Sciences. D.G. thanks AT&T Bell Laboratories for its hospitality.

APPENDIX A: STABILITY OF CLUSTER STATES

In order to check if a limit cycle is stable, one has to find the eigenvalues of the operator $U(T_p)$ [Eqs. (2.16) and (2.15)]. Generally, this is a complicated problem. The situation simplifies if there exists a set of vectors $\{\mathbf{v}_n\}$ which are eigenvectors of the matrix M for *any* point $\phi(t)$ along the trajectory. The eigenvalues $\mu_n(\phi)$ corresponding to these eigenvectors can vary from point to point. These global eigenvectors span a subspace V_{\parallel} . In this basis $U(T_p)$ is diagonal in V_{\parallel} . Its diagonal elements are

$$[U(T_p)]_{n,n} = I_n = \int_0^{T_p} dt \mu_n(\phi(t)). \quad (\text{A1})$$

The subspace orthogonal to V_{\parallel} is denoted by V_{\perp} . Calculating the matrix elements of $U(T_p)$ in this subspace is still a difficult task.

We apply this method now to the N_c -cluster state, with $\epsilon_k N$ oscillators in the k th cluster. The matrix M is built from blocks:

$$M = \begin{pmatrix} \tilde{M}_{11} & \tilde{M}_{12} & \cdots & \tilde{M}_{1N_c} \\ \vdots & \ddots & & \vdots \\ \tilde{M}_{N_c 1} & \tilde{M}_{N_c 2} & \cdots & \tilde{M}_{N_c N_c} \end{pmatrix}. \quad (\text{A2})$$

The diagonal block \tilde{M}_{kk} is a $\epsilon_k N \times \epsilon_k N$ square matrix:

$$\tilde{M}_{kk} = \begin{pmatrix} \frac{\partial f}{\partial \phi}(\Phi_k) - \frac{1}{N} \frac{\partial g}{\partial \phi}(\Phi_k) & -\frac{1}{N} \frac{\partial g}{\partial \phi}(\Phi_k) & \cdots & -\frac{1}{N} \frac{\partial g}{\partial \phi}(\Phi_k) \\ \vdots & \ddots & & \vdots \\ -\frac{1}{N} \frac{\partial g}{\partial \phi}(\Phi_k) & -\frac{1}{N} \frac{\partial g}{\partial \phi}(\Phi_k) & \cdots & \frac{\partial f}{\partial \phi}(\Phi_k) - \frac{1}{N} \frac{\partial g}{\partial \phi}(\Phi_k) \end{pmatrix}. \quad (\text{A3})$$

The nondiagonal block \tilde{M}_{kl} is a $\epsilon_k N \times \epsilon_l N$ matrix which has all its elements equal to $(1/N)(\partial g / \partial \phi)(\Phi_l)$. Each diagonal block is a cyclic matrix and can be diagonalized by Fourier transform. The m th component of the n_k th eigenvector of the k th diagonal block is

$$(v_{n_k})_m = \exp \left[\frac{2\pi i n_k m}{\epsilon_k N} \right],$$

$$n_k = 0, \dots, \epsilon_k N - 1, \quad m = 1, \dots, \epsilon_k N. \quad (\text{A4})$$

The corresponding eigenvalues of the diagonal block are $\mu_{n_k} = (\partial f / \partial \phi)(\Phi_k)$ for $1 \leq n_k \leq \epsilon_k N - 1$ and $\mu_0 = (\partial f / \partial \phi)(\Phi_k) - (\partial g / \partial \phi)(\Phi_k)$.

Corresponding to the block matrix M , we define an N -dimensional vector $\mathbf{V}_k^{n_k}$ with N_c segments, where the k th segment has $\epsilon_k N$ components. The components of all the segments are zero except the component of one segment, the k th. This segment is equal to one of the vectors v_{n_k} with $n_k \geq 1$. The vector $\mathbf{V}_k^{n_k}$ is an eigenvector of the matrix M with an eigenvalue $\mu_k^{n_k} = (\partial f / \partial \phi)(\Phi_k)$ and corresponds to an intracluster nonuniform fluctuation which tends to destroy the spatial cluster structure. Using Eq. (A1), it is seen that it is also an eigenvector of $U(T_p)$, with eigenvalue

$$I_k = \int_0^{T_p} dt \frac{\partial f(\Phi_k(t))}{\partial \Phi_k}. \quad (\text{A5})$$

There are $N - N_c$ such vectors that span the subspace V_{\parallel} , which has N_c different eigenvalues. Thus the N_c -cluster state is stable to intracluster fluctuations if, for all the clusters,

$$I_k < 0, \quad k = 1, \dots, N_c. \quad (\text{A6})$$

In order to compute I_k numerically, we have to know the trajectory. Thus we integrate Eq. (2.26) numerically for the N_c degrees of freedom, until it reaches the limit cycle. Since N_c is small in our model, this integration is much less time consuming than simulating the full system.

In particular, for one cluster (HLC) there is only one stability condition that can be written, using (2.24), (A6), and (A5), as

$$I_1 = \int_0^{2\pi} d\phi \frac{\partial f(\phi)}{\partial \phi} \frac{1}{\omega + f(\phi) - g(\phi)} < 0. \quad (\text{A7})$$

We do not have a simple way to calculate the intercluster fluctuations (for $N_c \geq 2$). However, we use the results of the numerical integration of Eq. (2.26) and say that if the system of N_c degrees of freedom converges to a limit cycle, it must be stable in the N_c -dimensional space of the clusters, and thus it should be stable in the N -dimensional space to intercluster fluctuations.

APPENDIX B: STABILITY ANALYSIS OF THE STATIONARY DISTRIBUTION AT $T=0$

The stationary distribution when $T=0$ is

$$P_s(\phi) = \frac{\nu}{\tilde{\omega} + f(\phi)}, \quad (\text{B1})$$

where ν and $\tilde{\omega}$ are determined self-consistently from the normalization condition (2.8) and Eq. (2.30). Linearizing the continuity equation (2.5) around $P_s(\phi)$, one writes $\partial(\delta P) / \partial t = L \delta P$, where the operator L is defined by

$$L \delta P(\phi, t) = - \frac{\partial}{\partial \phi} \{ [\tilde{\omega} + f(\phi)] \delta P(\phi, t) \} + \frac{\partial P_s(\phi)}{\partial \phi} \int_0^{2\pi} d\phi' g(\phi') \delta P(\phi', t). \quad (\text{B2})$$

The linear stability of $P_s(\phi)$ depends on the spectrum of eigenvalues of L . A convenient basis to solve the eigenproblem for L is provided by the functions $e^{2\pi i n G(\phi)}$, where

$$G(\phi) = \int_0^{\phi} d\phi' P_s(\phi'). \quad (\text{B3})$$

Expanding $\delta P(\phi, t) / P_s(\phi)$ on this basis

$$\frac{\delta P(\phi, t)}{P_s(\phi)} = \sum_{n=-\infty}^{\infty} a_n e^{2\pi i n G(\phi)}, \quad (\text{B4})$$

and substituting in Eq. (B2), one finds that

$$\dot{a}_n(t) = -2\pi i n \nu a_n(t) + b_n \sum_{m=-\infty}^{\infty} f_m a_m(t), \quad (\text{B5})$$

where

$$b_n = \int_0^{2\pi} d\phi \frac{dP_s(\phi)}{d\phi} e^{-2\pi i n G(\phi)} \quad (\text{B6})$$

and

$$f_m = \int_0^{2\pi} d\phi g(\phi) P_s(\phi) e^{2\pi i m G(\phi)}. \quad (\text{B7})$$

The spectrum of L is found by diagonalizing the matrix N_{nm} :

$$N_{nm} = -2\pi i n \nu \delta_{nm} + b_n f_m. \quad (\text{B8})$$

In the specific case $f(\phi) = A \sin \phi$, in which the stationary distribution is given by Eq. (3.10), we evaluated the integrals (B6) and (B7). From (B3) and (B1) one can see that, in this case,

$$\frac{d\phi}{dG} = \frac{\tilde{\omega}}{\nu} + \frac{A}{\nu} \sin \phi(G). \quad (\text{B9})$$

Therefore

$$\phi(G) = 2 \arctan \left[\frac{2\pi \nu}{\tilde{\omega}} \tan[\pi(G - G_1)] - \frac{A}{\tilde{\omega}} \right], \quad (\text{B10})$$

where G_1 is determined from the boundary condition $\phi(G=0)=0$. Using Eqs. (B10), (3.11), and (B9), one obtains the identities

$$\begin{aligned} \sin[\phi(G)] &= \frac{2 \tan[\phi(G)/2]}{1 + \tan^2[\phi(G)/2]} \\ &= \frac{-A + \tilde{\omega} \sin[2\pi(G - \hat{G})]}{\tilde{\omega} - A \sin[2\pi(G - \hat{G})]}, \end{aligned} \quad (\text{B11})$$

$$\begin{aligned} \cos[\phi(G)] &= \frac{1 - \tan^2[\phi(G)/2]}{1 + \tan^2[\phi(G)/2]} \\ &= \frac{(\tilde{\omega}^2 - A^2)^{1/2} \cos 2\pi(G - \hat{G})}{\tilde{\omega} - A \sin[2\pi(G - \hat{G})]}, \end{aligned} \quad (\text{B12})$$

$$\left[\frac{d\phi}{dG} \right]^{-1} = \frac{v\bar{\omega}}{\bar{\omega}^2 - A^2} - \frac{vA}{\bar{\omega}^2 - A^2} \sin[2\pi(G - \hat{G})], \quad (\text{B13})$$

where

$$\hat{G} = \frac{1}{2\pi} \arctan[-A/(\bar{\omega}^2 - A^2)^{1/2}]. \quad (\text{B14})$$

Integrating Eq. (B6) by parts and substituting (B13) and (3.11) in it, one obtains

$$\begin{aligned} b_n &= 2\pi i n \int_0^{2\pi} d\phi \left[\frac{dG(\phi)}{d\phi} \right]^2 e^{-2\pi i n G(\phi)} \\ &= \frac{2\pi i n v}{\bar{\omega}^2 - A^2} \int_0^1 dG e^{-2\pi i n G} \{ \bar{\omega} - A \sin[2\pi(G - \hat{G})] \} \\ &= \frac{-nA}{2(\bar{\omega}^2 - A^2)^{1/2}} (e^{-2\pi i n \hat{G}} \delta_{n,1} - e^{2\pi i n \hat{G}} \delta_{n,-1}). \end{aligned} \quad (\text{B15})$$

Since $b_n = 0$ for $|n| \neq 1$, the matrix N_{nm} has a set of left eigenvectors \mathbf{a}_l^T , $|l| \neq 1$, whose m th components is $\mathbf{a}_l^T(m) = \delta_{lm}$. The corresponding eigenvalues are

$$\lambda_l = -2\pi i v l, \quad |l| \neq 1. \quad (\text{B16})$$

In addition to these eigenvalues, there are two extra eigenvalues $\lambda_{\pm 1}$. In order to calculate them, one diagonalizes the restriction of L on a supplementary two-dimensional subspace, which is the matrix

$$\begin{bmatrix} -2\pi i v + b_1 f_1 & b_1 f_{-1} \\ b_{-1} f_1 & 2\pi i v + b_{-1} f_{-1} \end{bmatrix}. \quad (\text{B17})$$

The eigenvalues $\lambda_{\pm 1}$ were calculated explicitly in the case $g(\phi) = \sigma \sin(\phi + \alpha)$. Using Eqs. (B11), (B12), (3.11), and

$$\begin{aligned} &\int_0^1 \frac{e^{2\pi i m G}}{\bar{\omega} - A \sin(2\pi G)} dG \\ &= \frac{i^m}{(\bar{\omega}^2 - A^2)^{1/2}} \left[\frac{\bar{\omega} - (\bar{\omega}^2 - A^2)^{1/2}}{A} \right]^m, \quad m \geq 0, \end{aligned} \quad (\text{B18})$$

one can write

$$\begin{aligned} f_m &= i^{m-1} e^{2\pi i m \hat{G}} (\bar{\omega}^2 - A^2)^{1/2} \\ &\times \frac{[\bar{\omega} - (\bar{\omega}^2 - A^2)^{1/2}]^m}{A^{m+1}} (\sin\alpha + i \cos\alpha), \quad m > 0. \end{aligned} \quad (\text{B19})$$

$$f_{-m} = f_m^*.$$

Substituting (B15) and (B19), it is found that the characteristic equation of matrix (B17) is

$$\begin{aligned} \lambda^2 + \lambda \frac{\sigma}{A} [\bar{\omega} - (\bar{\omega}^2 - A^2)^{1/2}] \sin\alpha + \frac{\sigma}{A} (\bar{\omega}^2 - A^2)^{1/2} \\ \times [\bar{\omega} - (\bar{\omega}^2 - A^2)^{1/2}] \cos\alpha + \bar{\omega}^2 - A^2 = 0. \end{aligned} \quad (\text{B20})$$

The two roots of this equation, λ_{+1} and λ_{-1} , have both a negative real part if and only if

$$\lambda_{+1} + \lambda_{-1} = -\frac{\sigma}{A} [\bar{\omega} - (\bar{\omega}^2 - A^2)^{1/2}] \sin\alpha < 0, \quad (\text{B21})$$

$$\begin{aligned} \lambda_{+1} \lambda_{-1} &= \frac{\sigma}{A} (\bar{\omega}^2 - A^2)^{1/2} [\bar{\omega} - (\bar{\omega}^2 - A^2)^{1/2}] \cos\alpha \\ &\quad + \bar{\omega}^2 - A^2 \\ &> 0. \end{aligned} \quad (\text{B22})$$

If $\bar{\omega} > 0$, Eqs. (B21) and (3.2) yield $\sigma > 0$. In this case Eq. (B22) is always satisfied if $\cos\alpha \geq 0$. If $\sigma > 0$ and $\cos\alpha < 0$, then Eq. (B22) is satisfied if

$$\bar{\omega}^2 (A - 2\sigma \cos\alpha) > A(\sigma \cos\alpha - A)^2. \quad (\text{B23})$$

Using Eqs. (B23), (3.12), and (3.11), the following inequality is obtained:

$$\begin{aligned} (A^2 + 2\sigma^2 \cos^2\alpha - 2A\sigma \cos\alpha)(\bar{\omega}^2 - A^2 + 2A\sigma \cos\alpha)^{1/2} \\ > 2\omega(A - \sigma \cos\alpha)\sigma \cos\alpha, \end{aligned} \quad (\text{B24})$$

which holds automatically because the left-hand side is positive and the right-hand side is negative. Similar analysis shows that if $0 < \alpha < \pi$, the SD with $\bar{\omega} < 0$ has always one eigenvalue with a positive real part. Thus the two roots of Eq. (B20) have a negative real part [in the regime defined in (3.2)] if and only if

$$\sigma > 0 \quad \text{and} \quad \bar{\omega} > 0. \quad (\text{B25})$$

APPENDIX C: THE STATIONARY DISTRIBUTION AND ITS STABILITY AT $T > 0$

The stationary distribution at finite T is calculated by solving Eq. (4.8). $P_s(\phi)$ is expanded in the Fourier basis

$$P_s(\phi) = \frac{1}{2\pi} \sum_{n=-\infty}^{\infty} K_n e^{-in\phi}. \quad (\text{C1})$$

Substituting Eq. (C1) in Eq. (4.8) yields

$$\begin{aligned} (\bar{\omega} + inT) + \sum_{m=1}^{\infty} \frac{A_m}{2i} (e^{i\psi_m} K_{n+m} - e^{-i\psi_m} K_{n-m}) \\ = 2\pi v \delta_{n0}. \end{aligned} \quad (\text{C2})$$

This infinite set of linear equations is truncated, and only n_0 modes are kept. The resulting finite set of equations is solved numerically self-consistently with Eq. (2.6) for $\bar{\omega}$ and with the normalization condition $K_0 = 1$. The SD is calculated numerically as follows: Using an initial guess for $\bar{\omega}$, the distribution is calculated by solving Eq. (C2). Then a new guess for $\bar{\omega}$ is calculated by substituting the new distribution in Eq. (2.6) and vice versa. The process continues until $\bar{\omega}$ converges to a fixed value.

The stability of the SD is analyzed by diagonalizing the operator L :

$$\begin{aligned} L \delta P(\phi, t) &= -\frac{\partial}{\partial \phi} \{ [\bar{\omega} + f(\phi)] \delta P(\phi, t) \} \\ &\quad + \frac{\partial P_s(\phi)}{\partial \phi} \int_0^{2\pi} d\phi' g(\phi') \delta P(\phi', t) \\ &\quad + T \frac{\partial^2 [\delta P(\phi, t)]}{\partial \phi^2}. \end{aligned} \quad (\text{C3})$$

When $T \neq 0$ it is more convenient to use the standard Fourier basis than the specific basis that was described in Appendix B. Expanding $\delta P(\phi, t)$ in the Fourier basis

$$\delta P(\phi, t) = \frac{1}{2\pi} \sum_{n=-\infty}^{\infty} c_n(t) e^{-in\phi} \quad (\text{C4})$$

and substituting Eqs. (C4) and (C1) in Eq. (C3), we obtain

$$\begin{aligned} \dot{c}_n = & (in\bar{\omega} - Tn^2)c_n \\ & + \frac{n}{2} \sum_{m=1}^{\infty} A_m (e^{i\psi_m} c_{n+m} - e^{-i\psi_m} c_{n-m}) \\ & - \frac{n}{2} \sum_{m=1}^{\infty} \sigma_m (e^{i\alpha_m} c_m - e^{-i\alpha_m} c_{-m}) K_n. \end{aligned} \quad (C5)$$

The infinite-dimensional stability matrix defined by Eq. (C5) is approximated by a finite truncated $(2n_0+1) \times (2n_0+1)$ matrix, where n_0 is the number of modes that are taken into account. The finite matrix is diagonalized numerically. We chose n_0 to be 20. It was checked that increasing n_0 does not change significantly the part of the spectrum near zero, which is the more relevant part in the stability analysis.

*Permanent address: Racah Institute of Physics, The Hebrew University, Jerusalem 91904, Israel.

- [1] Y. Kuramoto, *Chemical Oscillations, Waves and Turbulence* (Springer, New York, 1984).
- [2] D. Fisher, *Phys. Rev. B* **31**, 1396 (1985); S. H. Strogatz, C. M. Marcus, R. M. Westervelt, and R. E. Mirollo, *Physica D* **36**, 23 (1989).
- [3] H. Sompolsky, D. Golomb, and D. Kleinfeld, *Proc. Natl. Acad. Sci. (U.S.A.)* **87**, 7200 (1990); *Phys. Rev. A* **43**, 6990 (1991).
- [4] Eckhorn *et al.*, *Biol. Cybern.* **60**, 121 (1988); C. M. Gray, P. König, A. K. Engel, and W. Singer, *Nature (London)* **338**, 334 (1989); A. K. Engel, P. König, C. M. Gray, and W. Singer, *Eur. J. Neurosci.* **2**, 558 (1990).
- [5] Y. Kuramoto and I. Nishikawa, *J. Stat. Phys.* **49**, 569 (1987).
- [6] H. Sakaguchi, S. Shinomoto, and Y. Kuramoto, *Prog. Theor. Phys.* **77**, 1005 (1987).
- [7] S. H. Strogatz and R. E. Mirollo, *J. Phys. A* **21**, L699 (1988); *Physica D* **31**, 143 (1988).
- [8] H. Sakaguchi, *Prog. Theor. Phys.* **79**, 39 (1988).
- [9] H. Daido, *J. Phys. A* **20**, L629 (1987); *Prog. Theor. Phys.* **77**, 622 (1987).
- [10] S. Shinomoto and Y. Kuramoto, *Prog. Theor. Phys.* **75**, 1105 (1986); H. Sakaguchi, S. Shinomoto, and Y. Kuramoto, *ibid.* **79**, 600 (1988).
- [11] K. Wiesenfeld and P. Hadley, *Phys. Rev. Lett.* **62**, 1335 (1989).
- [12] K. Y. Tsang, R. E. Mirollo, S. H. Strogatz, and K. Wiesenfeld, *Physica D* **48**, 102 (1991).
- [13] K. Kaneko, *Phys. Rev. Lett.* **63**, 219 (1989); *Physica D* **41**, 137 (1990); *Phys. Rev. Lett.* **65**, 1391 (1990).
- [14] L. Fabiny and K. Wiesenfeld, *Phys. Rev. A* **43**, 2640 (1991).
- [15] N. G. Van Kampen, *Stochastic Process in Physics and Chemistry* (North-Holland, Amsterdam, 1981), Chap. VIII.
- [16] S. H. Strogatz and R. E. Mirollo, *J. Stat. Phys.* **63**, 613 (1991).
- [17] P. Bergé, Y. Pomeau, and C. Vidal, *Order within Chaos* (Wiley, New York, 1984), p. 276.
- [18] H. Sompolsky, A. Crisanti, and H. J. Sommers, *Phys. Rev. Lett.* **61**, 259 (1988).
- [19] P. C. Matthews and S. H. Strogatz, *Phys. Rev. Lett.* **65**, 1701 (1990); P. C. Matthews, R. E. Mirollo, and S. H. Strogatz, *Physica D* **52**, 293 (1991).

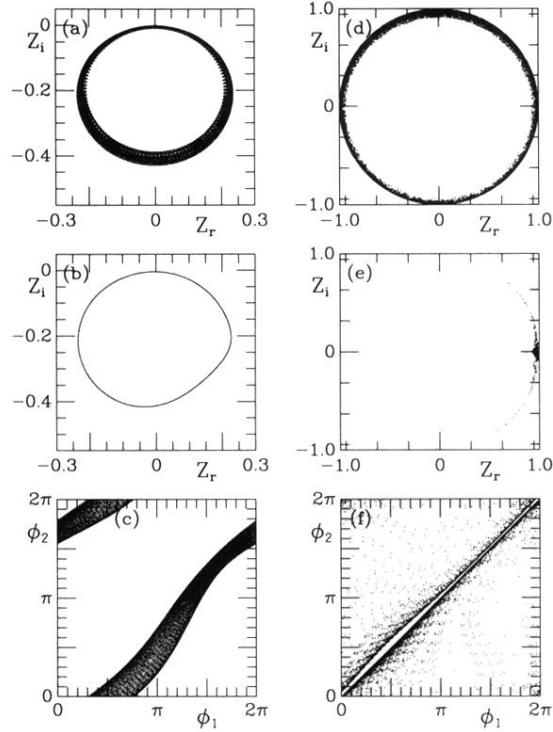


FIG. 3. Limit trajectory in the case $\omega=1$, $f(\phi)=0.5 \sin(\phi)$, and $g(\phi)=1.0 \sin(\phi+\alpha)$ obtained from simulating Eq. (2.1) with $N=100$. The system is in the marginal regime [Fig. 1(c)]. (a)–(c) The initial conditions are taken from uniform distribution. (a) The order parameter Z . (b) Poincaré section of the trajectory. It is obtained by plotting the value of Z every time when the phase ϕ_1 is zero. The Poincaré section is a close line, implying that the full trajectory is quasiperiodic with two basic frequencies. (c) Projection of the limit trajectory on the space of two oscillators ϕ_1 and ϕ_2 . (d)–(f) The initial conditions are taken from a Gaussian distribution with standard deviation 0.05. The motion is aperiodic. (d) The order parameter Z , (e) Poincaré section of the trajectory, and (f) projection of the limit trajectory on the space of two oscillators ϕ_1 and ϕ_2 .